

SUPPLEMENTARY INFORMATION

Elongated plant virus-based nanoparticles for enhanced delivery of thrombolytic therapies.

Andrzej S. Pitek,[†] Yunmei Wang,[‡] Sahil Gulati,^{§,||} Huiyun Gao,[‡] Phoebe L. Stewart,^{§,||} Daniel I. Simon,[‡] Nicole F. Steinmetz.^{*,†,⊥,#,¶,§}

[†] Department of Biomedical Engineering, Case Western Reserve University, Cleveland, OH 44106, USA

[‡] Harrington Heart & Vascular Institute, Case Cardiovascular Research Institute, Department of Medicine, University Hospitals Cleveland Medical Center and Case Western Reserve University School of Medicine, Cleveland, OH 44106, USA

[§] Department of Pharmacology, Case Western Reserve University, Cleveland, OH 44106, USA

^{||} Cleveland Center for Membrane and Structural Biology, Case Western Reserve University, Cleveland, OH 44106, USA

[⊥] Department of Radiology, Case Western Reserve University, Cleveland, OH 44106, USA

[#] Department of Materials Science and Engineering, Case Western Reserve University, Cleveland, OH 44106, USA

[¶] Department of Macromolecular Science and Engineering, Case Western Reserve University, Cleveland, OH 44106, USA

[§] Case Comprehensive Cancer Center, Division of General Medical Sciences-Oncology, Case Western Reserve University, Cleveland, OH 44106, USA

CONTENTS

- I. Figure S1. Model of STK interactions with PG and TMV.
- II. Figure S2. Cryo-EM imaging of TMV-PEG₈-STK and TMV-PEG₂₈-STK.
- III. Figure S3. Diffusion of molecules through fibrin matrix of *in vitro* phantom clots.
- IV. Movie S1. Movie of TMV-PEG₈-STK tomogram.
- V. Table S1. SDS-PAGE densitometry data for TMV-PEG₈-STK.
- VI. Table S2. SDS-PAGE densitometry data for TMV-PEG₂₈-STK.
- VII. Labeling of TMV and human serum albumins (HSA) with Cy5 fluorophores.

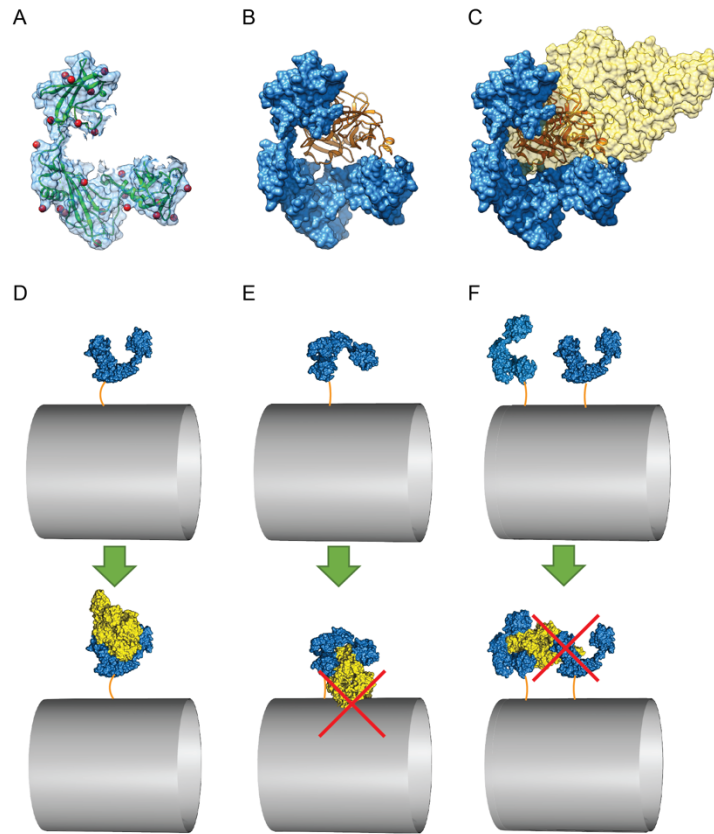


Figure S1. Model of STK interactions with PG and TMV. A) Model of STK structure and distribution of its 22 amine groups available for bioconjugation (indicated by red spheres). B) Structure of STK bound to catalytic domain of PG. C) Structure of full-size STK:PG active complex. D-E) To-scale model representation of three different scenarios of STK orientation on TMV surface, and its consequence for formation of STK:PG active complexes. TMV fragment is modeled by D=18 nm cylinder. STK is placed at ~4 nm distance from TMV surface, corresponding to maximum extension of -PEG₈- linker. Panel D) illustrates orientation of STK favorable for PG binding, while panels E&F demonstrate STK orientations that may impede PG binding due to steric hindrance with the TMV surface and neighboring STK molecules respectively. Structural data of proteins was obtained from PDB: i) STK complex with active domain of PG¹ (ID: 1BML), ii) full length type I human PG² (ID: 4DUU). Proteins were visualized and aligned using UCSF Chimera software.³

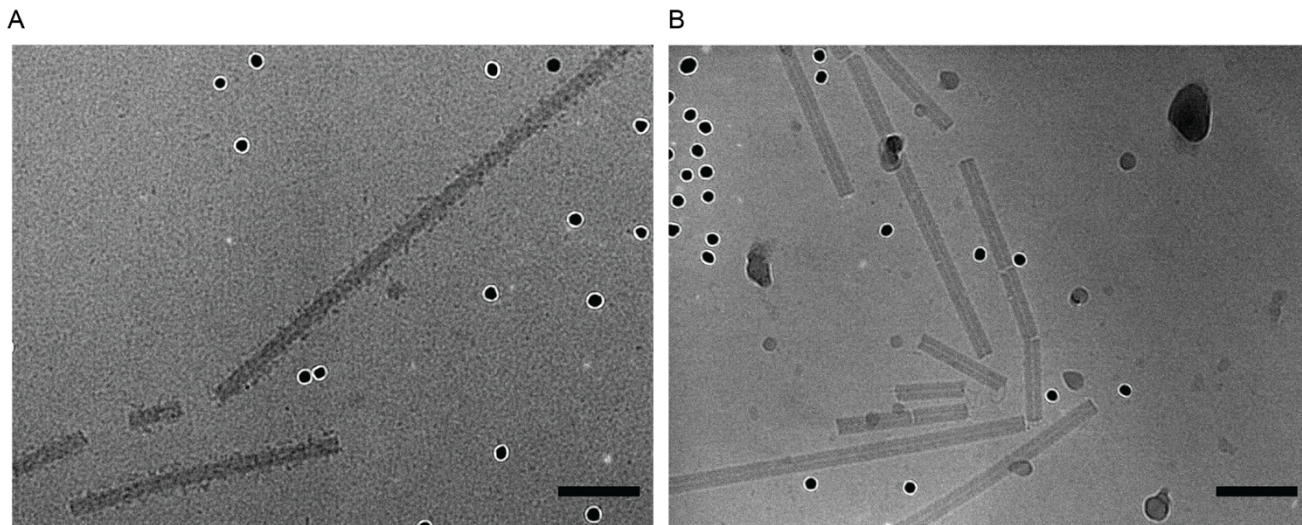


Figure S2. Cryo-EM imaging of TMV-PEG₈-STK and TMV-PEG₂₈-STK. A) Cryo-electron micrograph of TMV-PEG₈-STK showing densely packed STK molecules dotting the surface of the TMV particles. B) Cryo-electron micrograph of TMV-PEG₂₈-STK. A regular pattern of STK molecules is not observed on the surface of these TMV particles. The significantly lower surface coverage (6-9 \times) as compared to TMV-PEG₈-STK, and the greater variability in the end positions of the longer PEG linkers, make it difficult to identify density due to STK in this image. Several electron-dense 10nm nanogold fiducial markers are visible in the images. The scale bars represent 50 nm.

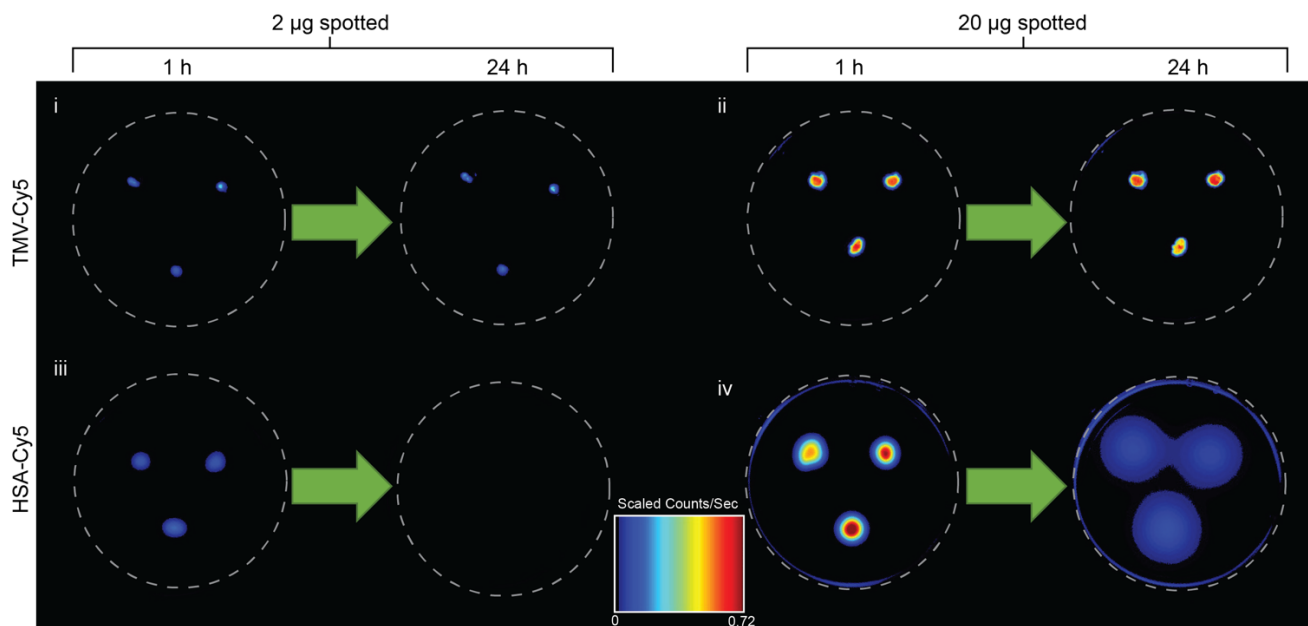
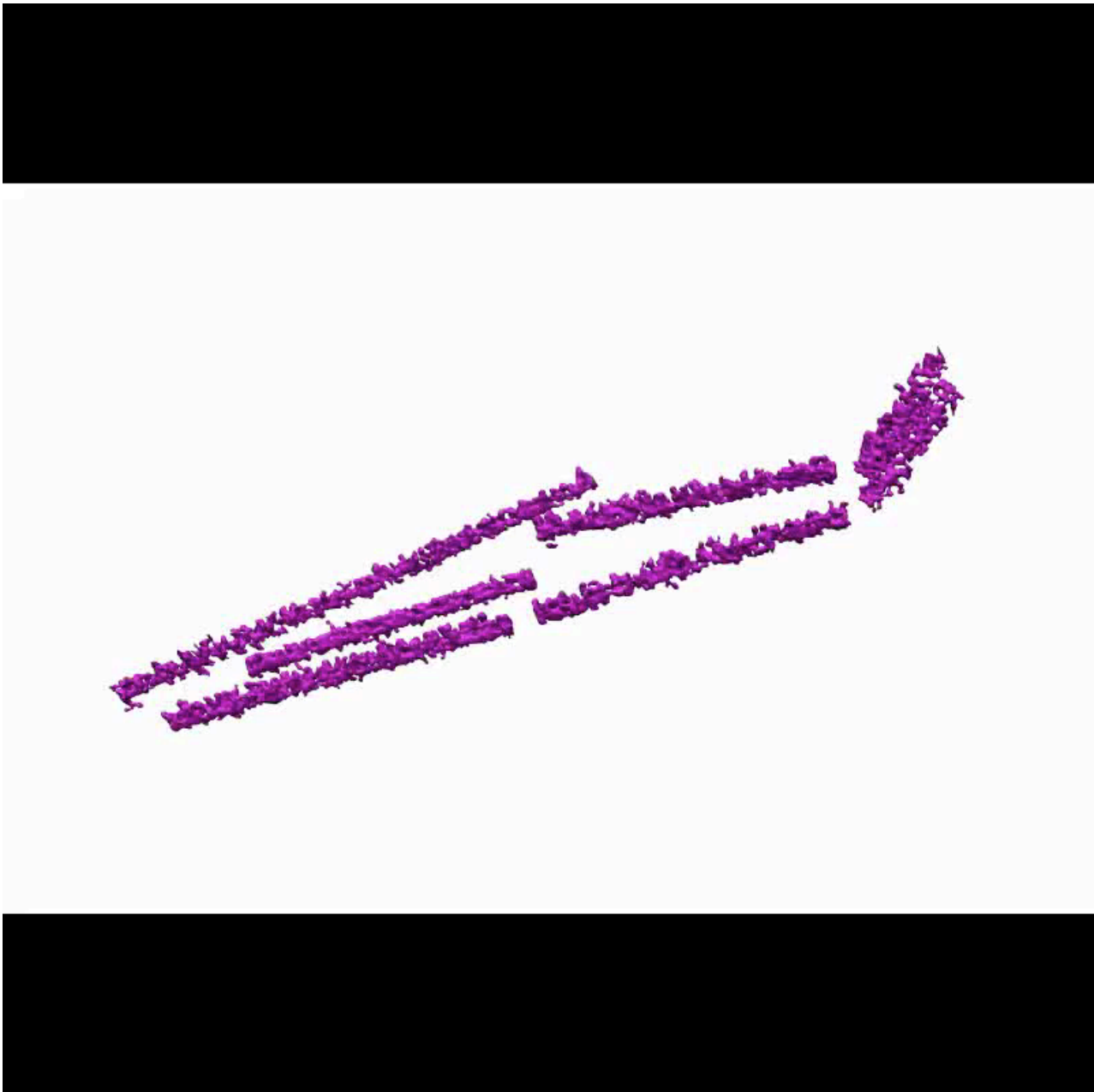


Figure S3. Diffusion of molecules through fibrin matrix of *in vitro* phantom clots. Fluorescently labeled TMV ($MW_{TMV}=3.94 \times 10^7$ Da) and HSA ($MW_{HSA} \sim 66$ kDa) were used as non-thrombolytic models of TMV-PEG_{8/28}-STK and STK molecules respectively. HSA was used instead of STK to avoid thrombolytic activity, which would lead to break down of the fibrous matrix and thus would not allow an investigation of diffusion in the absence of drug activity. Samples were applied to phantom clots in varying amounts (2 and 20 μg); their fluorescence distribution was imaged after 1 and 24 hours. HSA was observed to diffuse through fibrin matrix over time. The dimensions of the TMV particle (backbone molecule of TMV-PEG_{8/28}-STK) appear to be too large for penetration of the fibrin matrix under static conditions and without drug activity. Lack of fluorescent signal of 2 μg HSA sample after 24 hours (iii) was caused by the drop of its concentration below detection threshold, due to diffusion.



Movie S1. Movie of TMV-PEG₈-STK tomogram. Three-dimensional tomogram displaying a 360-degree view of TMV-PEG₈-STK. The STK molecules are seen as randomly oriented protrusions on the TMV surface (complete movie file is uploaded separately).

Table S1. SDS-PAGE densitometry data for TMV–PEG₈-STK.

	Band density [AU]				Std. curve equation	$\mu\text{g STK} / 20 \text{ ug TMV}^*$	$\mu\text{g STK} / \text{mg TMV}$	Number of STK/TMV**
	STK 1 μg	STK 5 μg	STK 10 μg	STK conjugate				
Gel 1	3503.86	10591.87	15028.79	41756.81 ^a	$y=0.0006*x$	12.53	626.35	525.07
Gel 2	1962.99	7254.67	13644.73	30579.558 ^b	$y=0.0007*x$	21.41	1070.28	897.22
Gel 3	3231.26	10363.63	16900.14	34963.014 ^b	$y=0.0006*x$	20.98	1048.89	879.28
							Average	767.19
							SD	209.87

* calculated using the standard curve equation

** calculated using $Mw_{\text{STK}}=47 \text{ kDa}$ and $Mw_{\text{TMV}}=39400 \text{ kDa}$

^a 40 μg total loading of TMV-PEG₈-STK sample

^b 20 μg total loading of TMV-PEG₈-STK sample

Table S2. SDS-PAGE densitometry data for TMV–PEG₂₈-STK.

	Band density [AU]				Std. curve equation	$\mu\text{g STK} / 20 \text{ ug TMV}^*$	$\mu\text{g STK} / \text{mg TMV}$	Number of STK/TMV**
	STK 1 μg	STK 5 μg	STK 10 μg	STK conjugate				
Gel 1	3072.01	12296.10	19709.87	5605.92 ^b	$y=0.0005*x$	2.80	140.15	117.49
Gel 2	4212.15	13612.49	20856.07	5906.10 ^b	$y=0.0004*x$	2.36	118.12	99.02
Gel 3	1962.99	7254.67	13644.73	2295.36 ^b	$y=0.0007*x$	1.61	80.34	67.35
Gel 4	3231.26	10363.63	16900.14	6384.37 ^b	$y=0.0006*x$	3.83	191.53	160.56
							Average	111.10
							SD	38.93

* calculated using the standard curve equation

** calculated using $Mw_{\text{STK}}=47 \text{ kDa}$ and $Mw_{\text{TMV}}=39400 \text{ kDa}$

^b 20 μg total loading of TMV-PEG₂₈-STK sample

Labeling of TMV and HSA with Cy5 fluorophores. First, alkynes were attached to TMV's (internal) and HSA's (external) carboxylic acids using 100 e.q., per TMVcp, or 1000 e.q., per HSA, of propargylamine (P50900; Sigma Aldrich) and 50 e.q. of EDC (25 equivalents added at 0 and 16 h; E6383; Sigma Aldrich) in 100 mM HEPES buffer (pH 7.4), for TMV, or PBS (0.01 M phosphate buffer, 0.0027 M potassium chloride and 0.137 M sodium chloride, pH 7.4), for HSA; the reaction was allowed to proceed for 20 h. Second, an alkyne-azide click reaction was performed by adding 1 e.q., per TMVcp, or 20 e.q., per HSA, of sCy5-azide (B3330; Lumiprobe) in the presence of 1 mM CuSO₄ (AC423615000; Fisher), 2 mM AMG (AC36891025; Fisher), and 2 mM Asc (AC352681000; Fisher) in 10 mM potassium phosphate buffer (KP, pH 7.4), for TMV, or PBS (pH 7.4), for HSA, on ice for 30 min. TMV was purified by ultracentrifugation at 42,000 rpm for 3 h on a 40% (w/v) sucrose cushion in PBS followed by two washes in PBS and repeated ultracentrifugation steps over 40% (w/v) sucrose cushion. HSA was purified using PD MiniTrap G-25 desalting columns (28-9180-08; GE) for at least 4 times; until no free dye was detected in the sample.

References:

- (1) Wang, X., Lin, X., Loy, J. A., Tang, J., and Zhang, X. C. (1998) Crystal Structure of the Catalytic Domain of Human Plasmin Complexed with Streptokinase. *Science* 281, 1662–1665.
- (2) Law, R. H. P., Caradoc-Davies, T., Cowieson, N., Horvath, A. J., Quek, A. J., Encarnacao, J. A., Steer, D., Cowan, A., Zhang, Q., Lu, B. G. C., Pike, R. N., Smith, A. I., Coughlin, P. B., and Whisstock, J. C. (2012) The X-ray crystal structure of full-length human plasminogen. *Cell Rep* 1, 185–190.
- (3) Pettersen, E. F., Goddard, T. D., Huang, C. C., Couch, G. S., Greenblatt, D. M., Meng, E. C., and Ferrin, T. E. (2004) UCSF Chimera—a visualization system for exploratory research and analysis. *J Comput Chem* 25, 1605–1612.